Carbon monoxide dissociative attachment and resonant dissociation by electron-impact

V. Laporta[1,2,3,*], J. Tennyson[3] and R. Celiberto[4,2]
[1] *Ohio Aerospace Institute, Dayton 45431, Ohio, USA*
[2] *Istituto di Nanotecnologia, CNR, Bari, Italy*
[3] *Department of Physics and Astronomy, University College London, London WC1E 6BT, UK and*
[4] *Dipartimento di Ingegneria Civile, Ambientale, del Territorio, Edile e di Chimica, Politecnico di Bari, 70125 Bari, Italy*

Low-energy dissociative electron attachment and resonant electron impact dissociation of CO molecule are considered. Ro-vibrationally resolved cross sections and rate coefficients for both the processes are calculated using an *ab-initio* model based on the low-lying $X\,^2\Pi$ resonance of CO^-. Final results show that the cross sections increases very rapidly as a function of the ro-vibrational level; these cross sections should be useful for understanding kinetic dissociation of CO in strongly non-equilibrium plasmas.

Carbon monoxide is a very important molecule playing a fundamental role in many fields. It is, in fact, one of the most abundant species in interstellar medium and can act as a tracer for H_2 molecules, which, due to the lack of ground electronic state transition dipole moment, cannot be observed directly but is detected thorough collisions with CO molecules [1]. CO is present in the atmosphere of planets and comets. It is a component of Mars' and Venus' atmosphere and, in the latter case, represents the most abundant chemical species. It therefore plays a crucial role also in space missions in connection to the (re-)entry problems [2]. Carbon monoxide, finally, is also useful in the understanding of processes involved in CO laser [3].

In a recent article we published state-resolved cross sections for electron-impact vibrational excitation of carbon monoxide [4]. Those vibrational data are useful in general in plasma vibrational kinetics, where non-thermal conditions can overpopulate the high vibrational levels of CO molecule [5]. In particular, they have been recently used in modeling the cooling of electrons in non-equilibrium CO-containing flows (see *e.g.* Refs. [6–8]). Since dissociation is an important process in plasma kinetics, as it leads to the depopulation of the vibrational levels, in the present letter we wish to extend our previous work to dissociative electron attachment (DEA) and to resonant electron impact-dissociation (EID) of CO, taking place through the temporary formation of the resonance $CO^-(X\,^2\Pi)$. DEA is known to be a relevant process that produces stable negative ions of oxygen [9].

The reactions considered here, respectively for DEA and EID processes, are the following:

$$e + CO(X\,^1\Sigma^+; v, j) \rightarrow CO^-(X\,^2\Pi) \rightarrow C(^3P) + O^-(^2P)\,, \quad (1)$$

$$e + CO(X\,^1\Sigma^+; v, j) \rightarrow CO^-(X\,^2\Pi) \rightarrow e + C(^3P) + O(^3P)\,, \quad (2)$$

where v, j represent the quantum numbers for the ro-vibrationl levels of the ground electronic state of CO. The vibrationally excited CO molecules, in the DEA process, undergo

* vincenzo.laporta@nanotec.cnr.it

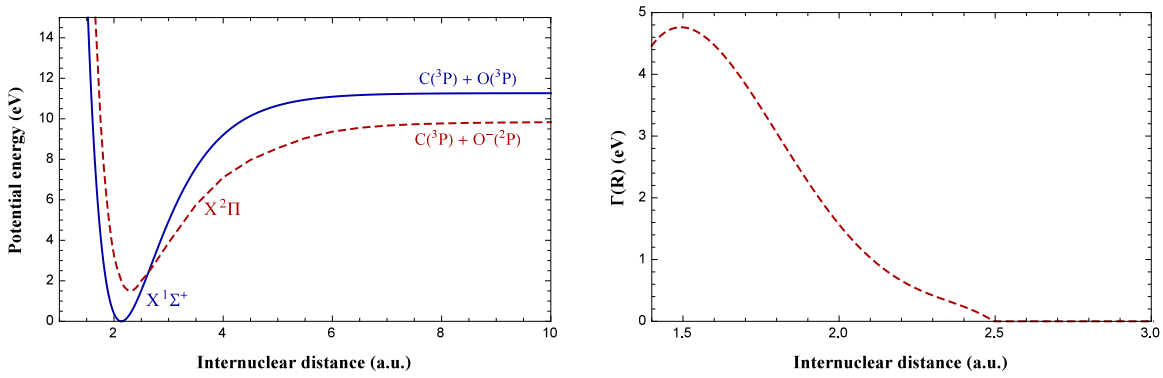

FIG. 1: Potential energy curves for the electronic ground state of CO and for the resonant state CO^- (left hand side) and the resonance width (right hand side) for $j = 0$ taken from Ref. [4].

dissociation with production of a negative oxygen ion while, in the EID process, they decay by emitting an electron which causes vibrational excitation ending in the vibrational continuum of the ground electronic state, then followed by molecular dissociation. The potential energy curves for the neutral and resonant species, CO and CO^-, respectively and the resonance width, $\Gamma(R)$, were obtained in Ref. [4] using MOLPRO [10] and the UK Molecular R-Matrix [11] *ab-initio* quantum chemistry codes. The results are displayed in Fig. 1. We calculated also the vibrational energy levels for the neutral molecule, up to dissociation, whose value are given in Table I for $j = 0$. Actually, in addition to the reactions displayed in Eqs. (1) and (2), there is a third dissociative channel which leads to the formation of $C^- + O$ in the final state. In the following, we neglect this state as the corresponding cross sections are several orders of magnitude lower than the DEA and EID as demonstrated by experimental measurements [12].

The cross sections for the reactions (1) and (2) for electron energy ϵ are given, respectively, by:

$$\sigma^{\rm DEA}_{v,j}(\epsilon) \;=\; 2\,\pi^2\,\frac{m_e}{k}\,\frac{K}{\mu}\,\lim_{R\to\infty}|\xi(R)|^2\;, \tag{3}$$

$$\sigma^{\rm EID}_{v,j}(\epsilon) \;=\; \frac{64\,\pi^5\,m_e^2}{\hbar^4}\int d\epsilon'\frac{k'}{k}\,|\langle\chi_{\epsilon'}(R)|\mathcal{V}|\xi(R)\rangle|^2\;, \tag{4}$$

where: K is the asymptotic momentum of the dissociating fragments C and O^- with reduced mass μ; m_e, $k = \sqrt{2m_e\epsilon/\hbar}$ and $k' = \sqrt{2m_e\epsilon'/\hbar}$ are the mass, the incoming and outgoing momentum of the electron; $\xi(R)$ is the solution of the Schrodinger-like equation for the resonant state and total energy $E = \epsilon_{v,j} + \epsilon$:

$$\left(-\frac{\hbar^2}{2\mu}\frac{d^2}{dR^2} + \frac{j(j+1)\hbar^2}{2\mu R^2} + V^- + \frac{i}{2}\Gamma - E\right)\xi(R) = -\mathcal{V}\,\chi_{v,j}(R)\,, \tag{5}$$

where $V^- + \frac{i}{2}\Gamma$ is the complex potential of the resonance, whose components are shown in Fig. 1; $\mathcal{V} = [\Gamma/(2\pi\,k)]^{1/2}$ is the discrete-to-continuum potential coupling and $\chi_{v,j}$ is the wave function of CO corresponding to the ro-vibrational level v, j. R represents the internuclear distance. In Eq. (4), $\langle\cdots\rangle$ means integration over the internuclear distance R and $\chi_{\epsilon'}$ is the continuum wave function of CO with energy ϵ' representing the C + O + e^- fragments. The integration on continuum energy ϵ' was carried out from CO dissociation threshold, D_e,

v	$\epsilon_{v,0}$ (eV)	v	$\epsilon_{v,0}$ (eV)	v	$\epsilon_{v,0}$ (eV)	v	$\epsilon_{v,0}$ (eV)
0	0.0000	20	4.8243	40	8.2869	60	10.3877
1	0.2735	21	5.0297	41	8.4243	61	10.4570
2	0.5437	22	5.2318	42	8.5582	62	10.5229
3	0.8104	23	5.4305	43	8.6888	63	10.5854
4	1.0738	24	5.6257	44	8.8160	64	10.6445
5	1.3337	25	5.8176	45	8.9397	65	10.7002
6	1.5902	26	6.0060	46	9.0601	66	10.7524
7	1.8434	27	6.1911	47	9.1771	67	10.8013
8	2.0931	28	6.3727	48	9.2906	68	10.8468
9	2.3394	29	6.5510	49	9.4008	69	10.8888
10	2.5823	30	6.7258	50	9.5075	70	10.9275
11	2.8218	31	6.8972	51	9.6109	71	10.9628
12	3.0580	32	7.0652	52	9.7108	72	10.9946
13	3.2907	33	7.2299	53	9.8073	73	11.0231
14	3.5200	34	7.3911	54	9.9005	74	11.0481
15	3.7459	35	7.5489	55	9.9902	75	11.0697
16	3.9684	36	7.7033	56	10.0765	76	11.0880
17	4.1874	37	7.8543	57	10.1594	77	11.1028
18	4.4031	38	8.0019	58	10.2389	78	11.1142
19	4.6154	39	8.1461	59	10.3150	79	11.1222
						80	11.1267

TABLE I: CO vibrational levels and the corresponding energies (relative to the state $v = 0$) for ground electronic state and for $j = 0$. The dissociation energies are $D_e = 11.266$ eV and $D_0 = 11.128$ eV.

up to 10 eV. A similar model was recently used to successfully study DEA and EID in O_2 [13, 14] and EID in N_2 [15].

Figures 2 and 3 summarize the results for $j = 0$. In particular, Fig. 2 (left panel) shows the DEA cross sections for some initial vibrational levels as a function of the incident electron energy. It is evident from the figures that the cross sections for $v = 0$ are very small but they increase rapidly for higher vibrational levels. The oscillatory structure is due to the overlap of the vibrational wave functions of the neutral and resonant state [16]. A similar situation is observed for the EID cross sections. Figure 3 (left panel) shows that the variation of the cross sections with the vibrational level of the molecule is even stronger than for DEA. The different threshold between the corresponding cross sections at fixed v of DEA and EID is due to the electron affinity of oxygen, $E_a = 1.46$ eV.

Both the right panels of Figures 2 and 3 show, as a function of the electron temperature T_e, the rate coefficients for the processes (1) and (2) calculated from the corresponding cross sections assuming a Maxwellian energy distribution for the plasma electrons, *i.e.*:

$$\mathrm{k}_{v,j}(T_e) = \frac{2}{\sqrt{\pi}} (\kappa T_e)^{-1.5} \int_{\epsilon_{th}}^{\infty} \epsilon \, \sigma_{v,j}(\epsilon) \, e^{-\epsilon/\kappa T_e} \, d\epsilon \,, \tag{6}$$

where κ is the Boltzmann constant and ϵ_{th} is the threshold energy of the process. The ab-

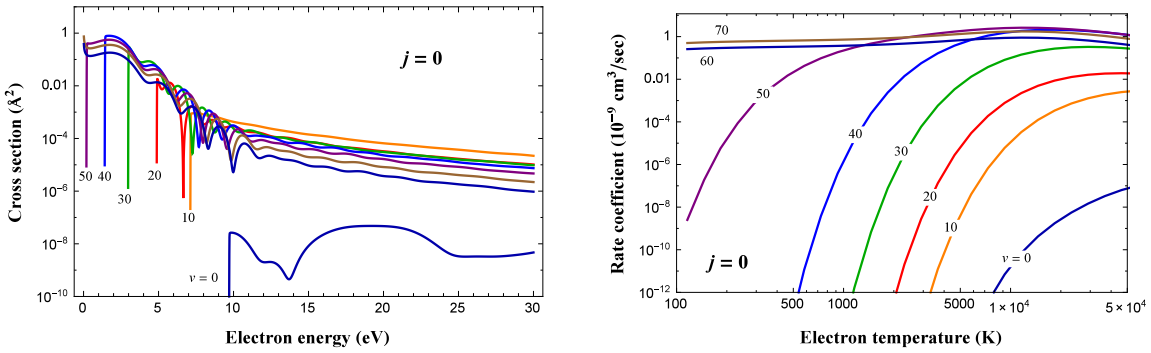

FIG. 2: Vibrational state-resolved dissociative electron attachment cross sections and the corresponding rate constants for $j = 0$.

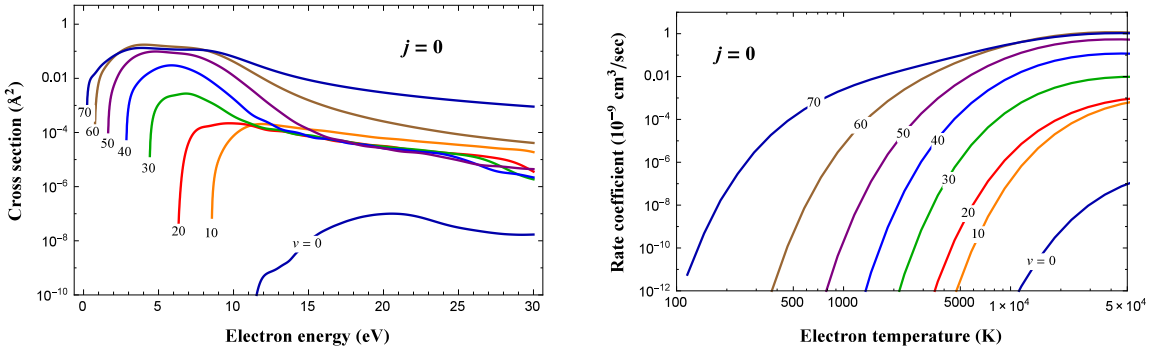

FIG. 3: Vibrational state-resolved electron-impact dissociation cross sections and the corresponding rate constants for $j = 0$.

solute value for rate coefficients grow monotonically as the vibrational level v increase and they become very large, particularly for $T_e > 1000$ K. These rates are important for models of plasmas in strong non-equilibrium. No experimental data are available for resonant dissociation while DEA has been measured by Rapp and Briglia [17] and recently reviewed by Itikawa [18] as part of his compilation of electron–CO cross sections. However the experimental data was obtained at room temperature using a thermal target which means that the small contribution to the process occurring from the $X\,^2\Pi$ resonance is obscured by the contribution coming from the $A\,^2\Sigma$ resonant state. DEA from the $A\,^2\Sigma$ resonance will be the subject of future work.

Cross sections for $j = 0$, basically, are valid at room temperature where rotational excitation is low. As the temperature increases rotational effects becomes more important. Fig. 4 shows the j-dependence of the $v = 0$ cross sections for both the DEA and EID processes. For low values of j, similar oscillatory behaviour to the case of vibration excitations is found. As the rotational quantum number increases, the potential energy curves, including the centrifugal contribution, become less deep and the corresponding cross sections increase in value while the threshold of the dissociative process is reduced. Dashed curves in Fig. 4 refer to the j-averaged cross sections obtained by assuming a rotational temperature $T_R = 10000$ K and $v = 0$:

$$\bar{\sigma}_v(T_R, \epsilon) = \sum_j \sigma_{v,j}(\epsilon)\,(2j+1)\,e^{-\epsilon_{v,j}/\kappa T_R}\,. \tag{7}$$

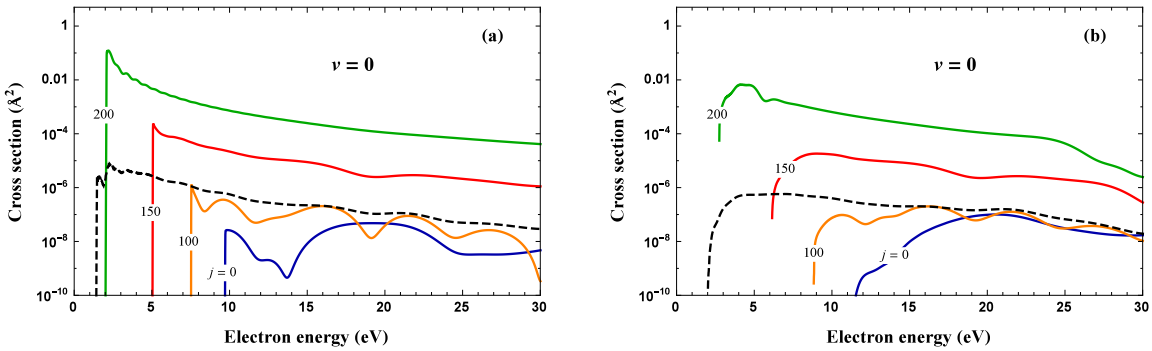

FIG. 4: Rotational state-resolved cross sections for $v = 0$: (a) dissociative electron attachment and (b) electron impact dissociation. Dashed black curves refer to the j-averaged cross sections calculated by assuming a rotational temperature of 10000 K.

In conclusion, in the present letter we have extended our previous work in Ref. [4] on vibrational excitation of CO molecule by electron-impact, by calculating the cross sections and the corresponding rates constants for the dissociative electron attachment and electron impact-dissociation processes. Understanding these processes is very important in modeling non-equilibrium plasma as they represent the principal reactions that lead to direct break of CO molecule antagonist to the so-called 'pure-vibrational-mechanism' for dissociation [7]. The full set of data obtained in the present work is available *via* the website of the Phys4Entry project [19] and as supplementary material to this letter.

Acknowledgments

The authors wish to thank Prof. M. Capitelli (University of Bari, Italy) for useful discussions. Research of V.L. was funded by Ohio Aerospace Institute, grant agreement project #WE202270.

References

[1] Eric B. Burgh, Kevin France, and Stephan R. McCandliss. *Astrophys. J.*, 658:446, 2007.
[2] L. Campbell, M. Allan, and M. J. Brunger. *J. Geophys. Res.*, 116:A09321, 2011.
[3] G.N. Haddad and H.B. Milloy. *Aust. J. Phys.*, 36:473, 1983.
[4] V Laporta, C M Cassidy, J Tennyson, and R Celiberto. *Plasma Sources Sci. Tech.*, 21:045005, 2012.
[5] Katherine A. Essenhigh, Yurii G. Utkin, Chad Bernard, Igor V. Adamovich, and J. William Rich. *Chem. Phys.*, 330:506 – 514, 2006.
[6] F. Graetz, D. P. Engelhart, R. J. V. Wagner, G. Meijer, A. M. Wodtke, and T. Schafer. *J. Chem. Phys.*, 141:044712, 2014.
[7] M. Capitelli, G. Colonna, G. D'Ammando, V. Laporta, and A. Laricchiuta. *Chem. Phys.*, 438:31 – 36, 2014.

[8] T. Kozak and A. Bogaerts. *Plasma Sources Sci. Tech.*, 24:015024, 2015.
[9] N L Aleksandrov and E M Anokhin. *J. Phys. D: Appl. Phys.*, 42:225210, 2009.
[10] H.-J. Werner, P. J. Knowles, G. Knizia, F. R. Manby, M. Schütz, et al. MOLPRO, version 2010.1, a package of ab initio programs, 2010.
[11] J. Tennyson. *Phys. Rep.*, 491:29 – 76, 2010.
[12] A. Stamatovic and G. J. Schulz. *J. Chem. Phys.*, 53:2663–2667, 1970.
[13] V. Laporta, R. Celiberto, and J. Tennyson. *Phys. Rev. A*, 91:012701, 2015.
[14] V. Laporta, R. Celiberto, and J. Tennyson. *AIP Conf. Proc.*, 1628:939–942, 2014.
[15] V Laporta, D A Little, R Celiberto, and J Tennyson. *Plasma Sources Sci. Tech.*, 23:065002, 2014.
[16] R. Celiberto, R. K. Janev, V. Laporta, J. Tennyson, and J. M. Wadehra. *Phys. Rev. A*, 88:062701, 2013.
[17] D. Rapp and D. D. Briglia. *J. Chem. Phys.*, 43:1480–1489, 1965.
[18] Y. Itikawa. *J. Phys. Chem. Ref. Data*, 44:013105, 2015.
[19] Database of the european union phys4entry project, 2012-2015. http://users.ba.cnr.it/imip/cscpal38/phys4entry/database.html.